Numerical solution of the hypernetted chain equation for a solute of arbitrary geometry in three dimensions

Dmitrii Beglov and Benoît Roux
Centre de Recherche en Calcul Appliqué (CERCA), Departments of Physics and Chemistry, University of Montreal, C.P. 6128, succ. Centre-Ville, Canada, H3C 3J7

(Received 18 January 1995; accepted 29 March 1995)

The average solvent distribution near complex solid substrates of arbitrary geometry is calculated by solving the hypernetted chain (HNC) integral equation on a three-dimensional discrete cubic grid. A numerical fast Fourier transform in three dimensions is used to calculate the spatial convolutions appearing in the HNC equation. The approach is illustrated by calculating the average solvent density in the neighborhood of small clusters of Lennard-Jones particles and inside a periodic array of cavities representing a simplified model of a porous material such as a zeolite. Molecular dynamics simulations are performed to test the results obtained from the integral equation. It is generally observed that the average solvent density is described accurately by the integral equation. The results are compared with those obtained from a superposition approximation in terms of radial pair correlation functions, and the reference interaction site model (RISM) integral equations. The superposition approximation significantly overestimates the amplitude of the density peaks in particular cases. Nevertheless, the number of the nearest neighbors around the clusters is well reproduced by all approaches. The present calculations demonstrate the feasibility of a numerical solution of HNC-type integral equations for arbitrarily complex geometries using a three-dimensional discrete grid. © *1995 American Institute of Physics*.

INTRODUCTION

Computer simulations of atomic models represent a powerful approach to study many-body systems.[1] However, properties of nonuniform systems such as the average solvent distribution in the neighborhood of a solid substrate, converges often very slowly due to the limited sampling and are difficult to obtain accurately. For example, to describe the solvation of a substrate of arbitrary shape immersed in a fluid composed of monoatomic particles, the nonuniform average solvent density $\rho(\mathbf{r})$ must be obtained at all point $\mathbf{r}$ in a three-dimensional space. Modern integral equation theories based on free energy density functionals represent a powerful alternative to computer simulations.[2–6] One well-known theory to describe the average solvent density in the neighborhood of a solid substrate is derived from the hypernetted chain (HNC) equation by taking the infinite dilution limit in the concentration of the solute (solid substrate),[7]

$$\rho(\mathbf{r})=\bar{\rho}\,\exp[-U(\mathbf{r})/k_BT+c\star\Delta\rho(\mathbf{r})], \tag{1}$$

where $\bar{\rho}$ is the bulk density, $U(\mathbf{r})$ is the perturbating potential acting on the solvent due to the solute, $c(\mathbf{r})$ is the direct correlation function of the unperturbed uniform bulk fluid, the symbol $\star$ represents a three-dimensional spatial convolution and $\Delta\rho(\mathbf{r})=\rho(\mathbf{r})-\bar{\rho}$ is the deviation from the bulk density. More sophisticated integral equation theories have also been proposed.[2–6] Since they possess the same basic structure, the present discussion will be restricted to Eq. (1).

Due to the core exclusion between the solute and the solvent particles, the perturbating potential $U(\mathbf{r})$ in Eq. (1) is typically constituted of a harsh repulsive part, and other smoothly varying contributions such as the van der Waals interactions. Expansion of the average solvent density $\rho(\mathbf{r})$ in terms of spherical harmonic functions provide an effective method to solve Eq. (1) when the shape of the solute or solid substrate is spherical or nearly spherical.[8–10] However, such expansions may not converge rapidly when the shape of the substrate is markedly nonspherical, e.g., in the case of clusters of particles, near rough surfaces, or inside complex cavities. To treat the case of a solid substrate of arbitrary geometry, we have solved Eq. (1) using a three-dimensional discrete grid. Although such an application of the HNC equation to calculate the average solvent density around a substrate of arbitrary geometry represents a straightforward extension of well-established methods,[7] we found no example of such calculations in the literature. The main purpose of this communication is thus to report on the feasibility of a theoretical approach based on a numerical solution of HNC-type integral equations on a three-dimensional discrete grid.

To illustrate the approach, the average solvent density was calculated for model substrates immersed in a liquid composed of monoatomic Lennard-Jones particles. Clusters composed of a small number of Lennard-Jones particles were considered. In addition, a periodic array of cavities representing a simplified model for a porous material such as a zeolite was also considered. The method and the computational details are described in the next section.

METHOD AND COMPUTATIONAL DETAILS

A single solute immersed in a uniform liquid constituted of monoatomic spherical particles is considered in the infinite dilution limit. It is assumed that the average solvent density is given by the HNC equation (1). The numerical solution of Eq. (1) involves a mapping of the average density $\rho(x,y,z)$ and of the potential $U(x,y,z)$ on a discrete grid, e.g., $\rho(x,y,z)\rightarrow\rho(i,j,k)$ and $U(x,y,z)\rightarrow U(i,j,k)$. A discrete grid with $N=128$ points with a spacing d of 0.15 Å

 0021-9606/95/103(1)/360/5/$6.00

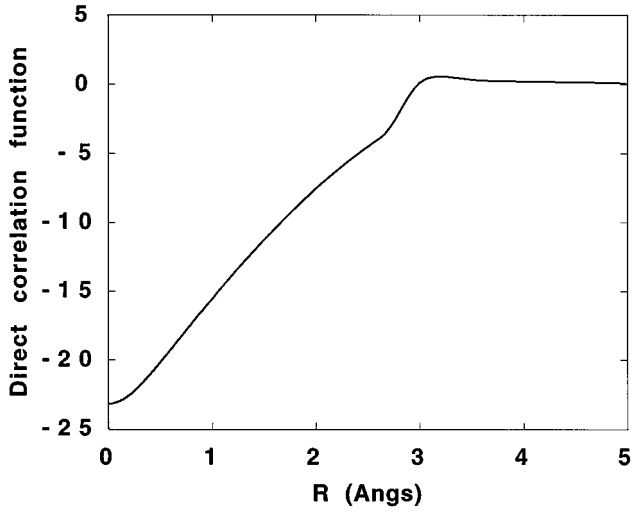

FIG. 1. Direct correlation function for the pure liquid obtained by solving the standard radial HNC equations (2)–(4). The Lennard-Jones parameters were $\sigma = 3.15066$ Å and $\epsilon = 0.152073$ kcal/mol.

was used in the calculations. The three-dimensional convolution $c \star \Delta\rho(\mathbf{r})$ in Eq. (1) was calculated using a numerical three-dimensional fast Fourier transform (FFT) procedure.[11] The convolution was calculated directly, without zero padding. This corresponds to a periodic system in the x, y, and z directions. The density and the temperature of the uniform fluid was 0.0334 Å^{-3} and 300 K, respectively. The value of the Lennard-Jones parameters of the fluid was $\sigma = 3.150663$ Å and $\epsilon = 0.152073$ kcal/mol, corresponding to a reduced density $\bar{\rho}\sigma^3$ of 1.04461 and reduced temperature $\epsilon/k_B T$ of 0.25541. The uniform fluid direct correlation function $c(r)$ used in all the calculations is shown in Fig. 1. It was obtained by solving the HNC equation for the neat liquid using the standard simplifications for spherically symmetric particles (radial HNC equation),[7]

$$c(r) = e^{-u(r)/k_B T + h(r) - c(r)} - 1 - [h(r) - c(r)] \tag{2}$$

and

$$\hat{h}(k) = \hat{c}(k) + (1 - \bar{\rho}\hat{c}(k))^{-1}, \tag{3}$$

where the Fourier transform of the radial functions ($c(r)$ and $h(r)$) is

$$\hat{f}(k) = 4\pi \int_0^\infty dr\ r^2 \frac{\sin(kr)}{kr} f(r). \tag{4}$$

An iterative scheme with simple mixing was used to solve the 3D HNC integral equation. The nth iteration is obtained from

$$\Delta\rho^{(n+1)} = \lambda\bar{\rho}\{\exp[-U/k_B T + c \star \Delta\rho^{(n)}] - 1\} + (1 - \lambda)\{\Delta\rho^{(n)}\}, \tag{5}$$

where λ is a mixing factor. Each iteration cycle involves the calculation of two three-dimensional FFT. In contrast with previous work,[8,9] the solute-solvent direct correlation function is not calculated in the present scheme and the iterations are done in terms of the deviation from the bulk density $\Delta\rho$ rather than the function $\eta = h - c$.

The 3D HNC equation was solved in the case of various solid substrates constructed from aggregates of Lennard-Jones particles having the same parameters σ and ϵ as those of the solvent. The average density in the neighborhood of small clusters, composed of 1–4 particles with interparticle separation distances of σ, was calculated. An interparticle separation of 1.2 Å was also considered for the two-particle substrate. The clusters were placed at the center of the grid. In addition, the average density inside a periodic array of cavities, a simplified model for a porous material such as a zeolite, was also calculated.

For comparison the average solvent density was also investigated using molecular dynamics (MD) simulations for the five solutes and model zeolite cavity. The dimension of the simulation cell is 18.631 Å and the systems contain 216 particles including those of the clusters, corresponding to a density of 0.0334 Å^{-3}. In the case of the model zeolite, the dimension of the periodic cell is 19.2 Å and 107 solvent molecules were included inside the cavities. This number was obtained by a volume integration of the solvent density calculated from the 3D HNC calculation of the same system. In all simulations periodic boundary conditions were applied in all directions. The configurational sampling was performed by generating a Langevin dynamics trajectory of 100 ps with a friction constant corresponding to a relaxation time of 25 ps^{-1}. During the simulations, strong harmonic restraints were used to keep the cluster particles at the designed distances. The particles forming the periodic array were held fixed in space. The trajectory was generated after 20 ps of equilibration. The trajectories were calculated using the CHARMM program.[12] The amplitude of the peaks of highest densities was calculated in an elementary volume from the trajectories using the symmetry of the cluster to improve the statistical convergence.

RESULTS AND DISCUSSION

To first test the feasibility of the numerical solution of Eq. (1) on a three-dimensional discretized grid, the average solvent distribution around a single Lennard-Jones particle is considered. The average solvent density along one of the grid axis through the center of the particle is shown in Fig. 2 along with the results obtained from the standard radial HNC equations (2)–(4). It is observed that the 3D HNC reproduces the correct density distribution accurately. A uniform bulk density $\bar{\rho}$ was taken as the initial guess for the iterational cycle. To stabilize the solution and reach convergence, it was necessary to initiate the cycle by performing 10 iterations with a mixing factor of 0.05 using Eq. (5). Then, 50 to 70 iterations with a mixing factor of 0.1 were used to reach convergence. In some cases, it was observed that the calculations would diverge with a larger mixing factor. The iteration cycle was repeated until the maximum difference of $[\rho^{(n+1)} - \rho^{(n)}]/\lambda\bar{\rho}$ over the whole grid was less than 4×10^{-4}. A grid spacing of 0.15 Å with 128 points, corresponding to an elementary cell of 19.2 Å , was necessary to get an acceptable accuracy in the 3D HNC calculations. Results obtained from a larger grid spacing did not reproduce the solution of radial HNC equation. The average density around the (2–4)-particle clusters was obtained using a simi-

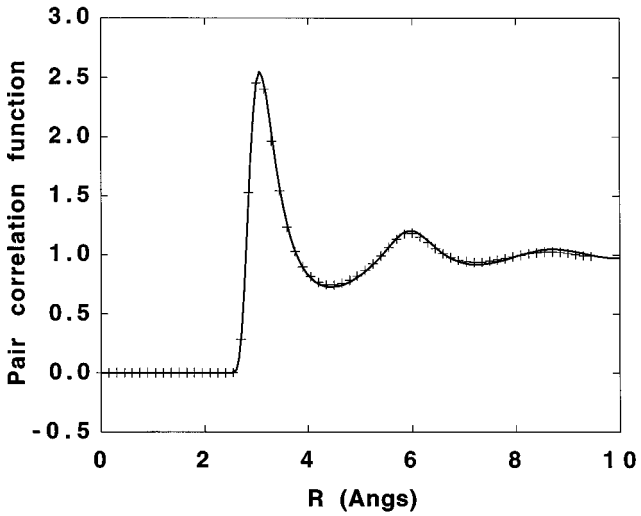

FIG. 2. The normalized radial distribution of the solvent around the 1-particle substrate (both with the same Lennard-Jones parameters). The solid line corresponds to the solution of the standard radial HNC equations (2)–(4). The crosses were obtained by numerical solution of Eq. (1) on a three-dimensional grid of $128\times128\times128$ points. A separation of 0.15 Å between the points was used.

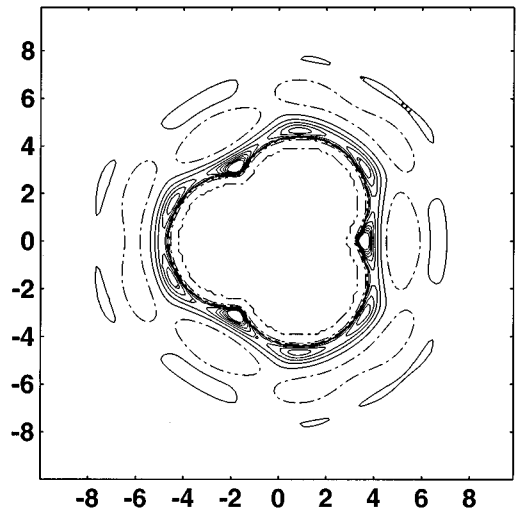

FIG. 4. Contour plot of the normalized radial distribution of the solvent in the plane of the 3-particle substrate with separation between substrate atoms equal to σ (dimensions along the axes are given in Å). The contours were drawn as in Fig. 3.

lar procedure with no difficulties. They are shown in Figs. 3, 4, and 5 (the case of the 4-particle cluster is difficult to represent clearly and is not shown).

The direct correlation function of the unperturbed bulk solvent, shown in Fig. 1, goes to zero at distances larger than 5 Å . This suggests that the short range character of $c(r)$ might have been exploited to evaluate the spatial convolution efficiently. However, the convolution is calculated several hundred times faster using the three-dimensional FFT procedure[11] than by performing a direct integration over the subvolume corresponding to the spatial extent of $c(r)$. The periodic boundary conditions used in the FFT have only a small influence on the solvent distribution calculated with the integral equation. For example, a small difference near 9 Å observed in Fig. 2 between the radial HNC and the 3*D* HNC is due to the periodicity introduced by the FFT in the three-dimensional convolutions. In addition, it is observed from the solvent distribution around the 3-particle substrate, shown in Figs. 4 and 5, that the amplitude and the width of secondary peaks are slightly affected and that there is a small loss of symmetry.

To assess the accuracy of the approach, it is necessary to compare the solvent distribution calculated with the 3*D* HNC equation to the results obtained from MD simulations. Im-

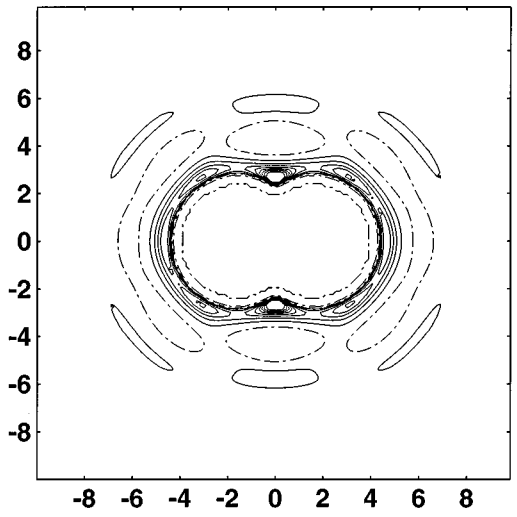

FIG. 3. Contour plot of the normalized radial distribution of the solvent in the plane of a 2-particle substrate with separation between substrate atoms equal to σ (dimensions along the axes are given in Å). The contours are plotted in the range of the normalized density from 0.0 to 4.0 with an increment 0.4. Dashed dotted lines are corresponding to density levels lower than the bulk one.

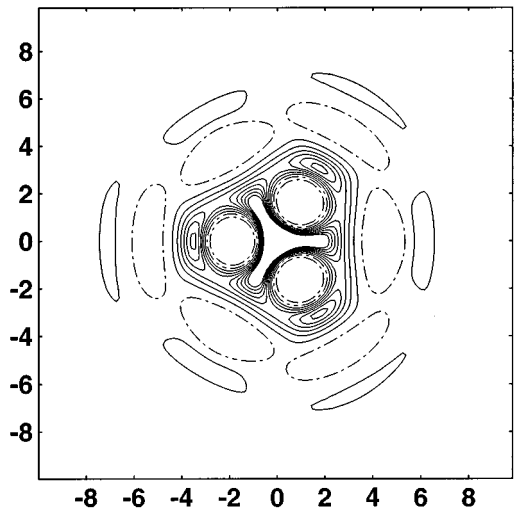

FIG. 5. Contour plot of the normalized radial distribution of the solvent in the x,y plane parallel to the 3-particle substrate located at $z=2.55$ Å (dimensions along the axes are given in Å). The absolute maximum of density around the cluster is located at $x=0$, $y=0$, and $z=2.55$. The contours were drawn as in Fig. 3.

TABLE I. Numbers and normalized maximal density of closest solvent molecules.

Solutes	Value	3D HNC	MD	SA	RISM
One particle	$N_1^{(1)}$	13.7	13.7	13.7	13.7
Two particles	$N_1^{(2)}$	12.6	12.7	12.7	12.7
1.2 Å apart	$N_2^{(2)}$	5.2	5.7	5.1	
	maximum density	5.9	5.4[b]	6.5	
Two particles[a]	$N_1^{(2)}$	13.9	14.0	14.2	13.8
	$N_2^{(2)}$	11.7	12.1	12.2	
	maximum density	3.2	2.82[c]	6.5	
Three particles[a]	$N_1^{(3)}$	11.6	11.5	11.6	11.7
	$N_2^{(3)}$	4.4	4.5	4.3	
	$N_3^{(3)}$	2.1	2.1	2.1	
	maximum density	12.1	11.5[d]	15.4	
Four particles[a]	$N_1^{(4)}$	10.5	10.6	10.8	10.8
	$N_2^{(4)}$	3.4	3.4	3.4	
	$N_3^{(4)}$	1.1	1.1	1.1	
	$N_4^{(4)}$	0.0	0.0	0.0	
	maximum density	12.6	11.4[e]	13.7	

[a]The distance between particles is equal to σ.
[b]Circular ring of the radius 2.65 Å and 0.15×0.15 Å^2 in a cross section lying in the middle plane between particles.
[c]Circular ring of the radius 3.09 Å and 0.15×0.15 Å^2 in a cross section lying in the middle plane between particles.
[d]Cubical volume element $0.15\times0.15\times0.15$ Å^3 placed 2.55 Å from the center of the triangle in the line going through the center of the triangle perpendicular to its plane.
[e]Cylindrical volume element of the radius 0.08463 Å and the height 0.15 Å placed 3.06 Å from the center of any triangle in the line going through the center of the triangle perpendicular to its plane from the opposite side of the fourth particle (it has the same volume as $0.15\times0.15\times0.15$ Å^3 cube).

portant features of the solvent distribution concern the number of cluster-solvent particle contacts and the position and the magnitude of the density peaks in the neighborhood of the clusters. To characterize the solvent distribution in the neighborhood of clusters composed of p particles, we define $N_m^{(p)}$, the average number of solvent particles that are simultaneously closer than 1.5σ from any m particles of the cluster ($m \leqslant p$). The main features of the solvent density around the five clusters obtained from the 3D HNC, and MD are summarized in Table I.

The numbers of neighboring solvent particles calculated by 3D HNC and by MD are very similar for all clusters. The value of the maximum density of the solute near all substrates calculated with the 3D HNC also agrees well with the maximum density estimated by MD. The number of solvent particles closest to a single cluster particle is approximately $N_1^{(p)} \approx N_1^{(p+1)} + 1$, i.e., addition of one particle in a p cluster (from p to $p+1$) has the effect of decreasing the number of solvent particles close to the other cluster particle by one. Structurally this means that the additional cluster particle occupies a region of space that was previously occupied by a solvent particle. Due to the packing, there is room for 14 neighbors around a central particle, corresponding to approximately 6 neighbors in a single plane going through the central particle. The consequences of this packing are observed in all the clusters. For example, the average density around the 2-particle cluster shown in Fig. 3 exhibits five peaks, the second particle of the cluster representing the sixth neighbor. Generally, the peaks of the highest density are found at the positions where a solvent particle can be in contact with the largest number of substrate particles. Peaks of high densities in the plane of the 3-particle substrate, shown in Fig. 4, are also at positions of a contact of two substrate particles, but the highest peak is at a distance of 2.55 Å above the plane of the triangle. The density in the plane going through this point (parallel to the 3-particle triangle) is shown in Fig. 5. The highest peak is the positions where a solvent particle can be in contact with the three particles of the cluster.

It is of interest to compare the 3D HNC solvent distribution with approximate schemes which are computationally attractive. An obvious candidate is the superposition approximation (SA), in which the average density at point $\mathbf{r}$ is expressed in terms of the radial pair correlation functions $g_i(r)$ of the ith individual solute centers,[7]

$$\rho(\mathbf{r}) = \bar{\rho} \prod_{i=1,m} g_i(|\mathbf{r}-\mathbf{r}_i|). \tag{6}$$

The reference interaction site model (RISM)[13] is a different approximation which is also used to treat the solvation properties of complex multicenter solutes constructed from radially symmetric interaction sites, e.g., molecular fluids[14] and polymers.[15] The results from SA and RISM are given in Table I for comparison with 3D HNC and MD. It is observed that the numbers of nearest solvent particles obtained by the SA are very similar to the results of the 3D HNC. A similar trend is observed for the 3- and 4-particle substrate. However, the SA overestimates the value of the maximum density. The error is largest in the case of the 2-particle substrate with a 1.2 Å separation where the maximum density is twice larger than the results of 3D HNC and MD. The number of nearest solvent particles $N_1^{(p)}$ obtained by the RISM are very similar to the results of the 3D HNC. It is not possible to further compare the RISM with the 3D HNC. Other characteristics of the three-dimensional solvent distribution are not available because the RISM framework allows only the calculation of reduced site-site solute-solvent radial distribution function around the individual cluster sites.[13] This analysis indicates that SA and RISM represent useful approximations for "integrated" characteristics, such as the average number of nearest neighbors. But the 3D HNC reproduces more accurately the magnitude and position of the density peaks than SA and provides more information than RISM on the spatial distribution of the solvent around the cluster.

Although the substrates that were considered above are nonspherical, they correspond to fairly localized perturbations on the bulk solvent. To provide a last illustration of the ability of the 3D HNC approach to treat arbitrary complex geometries, an infinite periodic array of Lennard-Jones particles, representing a simplified model for a porous material such as a zeolite, was considered. The model zeolite was constructed by putting Lennard–Jones particles on all the sites of a cubic lattice spaced by 2.13333 Å and by removing those that were inside the cylinders of diameter 3.5σ in the x, y, and z directions. The initial cell was constructed with nine particles in each direction. The resulting system, shown in Fig. 6, is a periodic array of cavities with communicating channels along the x, y, and z directions. The result of the

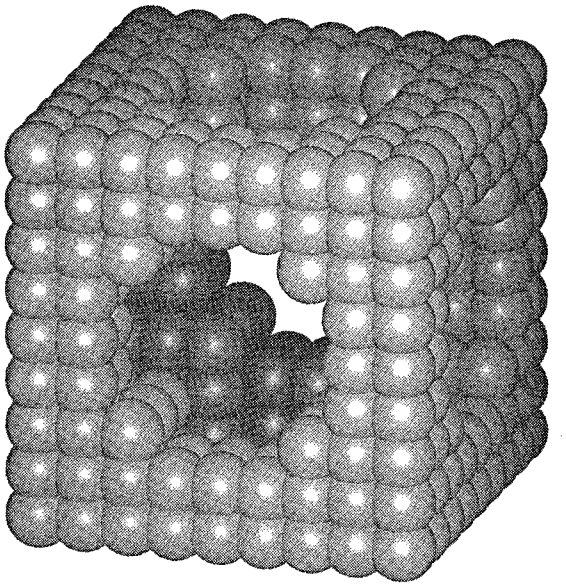

FIG. 6. Cubic unit cell of a material composed of Lennard-Jones particles representing a crude zeolite model.

calculation corresponds to the equilibrium solvent distribution that would arise inside the communicating cavities if the porous material was in contact with the bulk liquid. The normalized density averaged in cross sections perpendicular to the axis of any of the channels of the unit cell is shown in Fig. 7. The results from MD and SA are also shown for comparison. The density from 3*D* HNC and MD are in good agreement, whereas the SA greatly overestimates the density in several positions. The apparent complexity of the density profile along the channel would not have been predicted from simple arguments. Of course, the use of the direct correlation of the unperturbed bulk liquid is a very crude approximation in the case of a perturbation from an infinite solid substrate. Nevertheless, although the simple equation (1) may not be sufficiently accurate in the present case, the calculation provides an illustration of the ability of the approach to treat arbitrary complex geometries. More sophisticated density functional theories could be solved following a similar numerical approach to obtain better results.

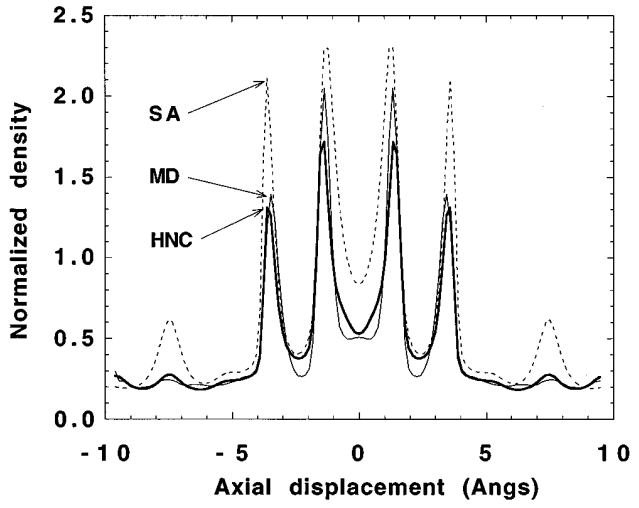

FIG. 7. Normalized projected solvent density along one axis of the model zeolite represented in Fig. 6. The results from the 3*D* HNC, MD, and SA are shown. In the case of MD, the density was calculated in a volume element between parallel planes 0.15 Å apart and the cubical symmetry of the unit cell was exploited to improve the statistical convergence.

CONCLUSION

It was demonstrated that the HNC equation can be solved numerically on a three-dimensional grid to calculate the average solvent distribution in the neighborhood of complex solid substrates of arbitrary geometries. The method was tested on various substrates models constructed from Lennard-Jones centers. Comparison with MD simulations indicate that the result of the integral equation is accurate. The present approach provides an alternative to computationally expensive MD simulations to obtain a detailed picture of the average solvent distribution near complex solid substrates. This could be useful to study fluid structure near rough surfaces or inside complex porous materials such as zeolites.

The present approach, illustrated here in the case of a simple monoatomic liquid, may be extended in various directions. For example, the accuracy of the HNC equation (1) may be improved by the introduction of reference bridge functions[8] or by using more sophisticated density functional theories developed to treat inhomogeneous fluids.[2–6] In addition, the method should be further developed to take the influence of orientational degrees of freedom of nonspherical solvent particles into account. Current approaches based on rotation matrix expansions should be readily applicable to the present situation.[8] Such extension is necessary to describing the electrostatic interactions present in a polar solvent. Further work is currently in progress in these directions.

ACKNOWLEDGMENT

Financial support was provided by NSERC.

[1] M. P. Allen and D. J. Tildesley, *Computer Simulation of Liquids* (Oxford Science, Clarendon, Oxford, 1989).
[2] C. Ebner, W. F. Saam, and D. Stroud, Phys. Rev. A **14**, 2264 (1976).
[3] W. F. Saam and C. Ebner, Phys. Rev. A **17**, 1768 (1978).
[4] R. Evans, P. Tarazona, and U. Marini Bettolo Marconi, Mol. Phys. **50**, 993 (1983).
[5] P. Tarazona and R. Evans, Mol. Phys. **52**, 847 (1984).
[6] R. Kjellander and S. Sarman, Mol. Phys. **70**, 215 (1990).
[7] J. P. Hansen and I. R. McDonald, *Theory of Simple Liquids* (Academic, London, 1976).
[8] P. H. Fries and G. N. Patey, J. Chem. Phys. **82**, 429 (1985).
[9] P. G. Kusalik and G. N. Patey, J. Chem. Phys. **88**, 7715 (1988).
[10] P. H. Fries, W. Kunz, P. Calmettes, and P. Turq, J. Chem. Phys. **101**, 554 (1994).
[11] W. H. Press, B. P. Flannery, S. A. Teukolsky, and W. T. Vetterling, *Numerical Recipes* (Cambridge University Press, Cambridge, 1990).
[12] B. R. Brooks, R. E. Bruccoleri, B. D. Olafson, D. J. States, S. Swaminathan, and M. Karplus, J. Comput. Chem. **4**, 187 (1983).
[13] D. Chandler and H. C. Andersen, J. Chem. Phys. **57**, 1930 (1972).
[14] D. Chandler and L. Pratt, J. Chem. Phys. **65**, 2925 (1976).
[15] C. J. Grayce, A. Yethiraj, and K. S. Schweizer, J. Chem. Phys. **100**, 6857 (1994).